Supporting Online Material for

A Basal Dinosaur from the Dawn of the Dinosaur Era in Southwestern Pangaea

Ricardo N. Martinez, Paul C. Sereno,* Oscar A. Alcober, Carina E. Colombi, Paul R. Renne, Isabel P. Montañez, Brian S. Currie

*To whom correspondence should be addressed. E-mail: dinosaur@uchicago.edu

Published 14 January 2011, *Science* **331**, 206 (2011)
DOI: 10.1126/science.1198467

This PDF file includes:

Materials and Methods

1—Material preserved
2—Measurements
3—Maturity assessment
4—Ischigualasto Formation: Stratigraphic summary
5—Ischigualasto Formation: $^{40}Ar/^{39}Ar$ geochronology
6—Phylogenetic analysis

1. Material preserved

1a. Holotype

The holotype of *Eodromaeus murphi* (PVSJ 560) is a nearly complete articulated skeleton. The cranium is disarticulated and flattened, exposing portions of both maxillae and dentaries in side view and the braincase in ventral view. The axial column is complete and articulated from the proatlas to the penultimate caudal vertebrae, except for portions of CA5 and 9, the intervening three vertebrae (CA6-8), a few of the vestigal caudal vertebrae at the distal tip of the tail, a few posterior cervical ribs, and gastralia. The appendicular skeleton is missing both scapulocoracoids, the distal ends of both humeri, the remainder of the right forelimb, the phalanges of left digit I, the distal end of the left ischium, the right astragalus and calcaneum, right metatarsals 4 and 5 and left metatarsals 2-4, and most pedal phalanges (Figure 2A).

1b. Referred material

PVSJ 534—Left femur, proximal right tibia, and a partially articulated left ankle and hind limb consisting of the astragalus, calcaneum, distal tarsal 3 and 4, and the proximal ends of metatarsals 1-4.

PVSJ 561—Articulated left maxilla, nasal and most of the jugal and right femur. The cranial piece was found on the underside of the block containing the holotype skeleton (PVSJ 560), and the femur was found a few centimeters away in the trench around the holotypic skeleton. It is possible they do not belong to the same individual.

PVSJ 562—Partial disarticulated skeleton including the posterior portion of the skull in articulation with the proatlas, atlas and cervical vertebrae 2-8 with associated ribs; isolated vertebrae including two mid dorsals (? D4, 6) and three posterior dorsals (? D11, 13, 14), an articulated series of nine anterior caudal vertebrae with chevrons (? CA2-10); left and right scapulocoracoids; an articulated left forelimb lacking manual phalanges distal to the proximal phalanx; left and right ischia lacking their distal ends; left femur, tibia and fibula and articulated right distal tibia, fibula, calcaneum and distal tarsal 4; and the distal end of metatarsal 4 in articulation with all phalanges of pedal digit IV. Found a few meters away from the holotype of *Eodromaeus murphi* (PVSJ 560).

PVSJ 877—Anterior cervical (? C3) centrum.

2. Measurements

The skull in *Eodromaeus* measures about 12 cm in length, based on a skull reconstruction assembled from cast bones of the holotype (PVSJ 560) and PVSJ 561

and on information on the form of the quadrate and braincase in PVSJ 562. Skull length was measured from the tip of the premaxilla to the posterior margin of the quadrate condyle.

The skeletal reconstruction (Fig. 2A) was based on the articulated skeleton of the holotype (PVSJ 560) and on fully prepared bones from PVSJ 562. Cervical, dorsal, sacral and caudal series are approximately 24, 35, 6, and 100 cm long, respectively. Total skeletal length measures approximately 177 cm. Measurements for individual bones for PVSJ 560 and 562 are given in Table S1.

Table S1. Skeletal measurements (mm) of the of the Late Triassic theropod *Eodromaeus murphi* nov. gen. nov. sp. Measurements are from the holotype (PVSJ 560) and the most complete referred specimen (PVSJ 562), which averages about 10-25% larger in dimension. Measurements of paired bones are from the right side except where indicated. Phalangeal length measures the functional chord, from the most invaginated point on the proximal articular socket to the apex of the distal articular condyle or tip of the ungual. Parentheses indicate estimated measurement. Abbreviations: *C*, cervical vertebra; *CA*, caudal vertebra; *D*, dorsal vertebra; *S*, sacral vertebra.

Bone **Measurement**	**PVSJ 560**	**PVSJ 562**
Cranium		
Cranium length (premaxilla to quadrate condyle)	(120)	—
Antorbital fossa maximum length	(41)	—
Quadrate height	—	38
Axial skeleton		
Proatlas length	—	13
C1 intercentrum length	—	4
C2 centrum length (without odontoid)	19	23
C3 centrum length	24	27
C4 centrum length	26	31
C5 centrum length	30	34
C6 centrum length	30	33
C7 centrum length	30	—
C8 centrum length	27	33
C9 centrum length	22	—
C10 centrum length	(13)	—
D1 centrum length	(15)	—
D2 centrum length	17	—
D3 centrum length	17	—
D4 centrum length	17	18[3]
D5 centrum length	17	—
D6 centrum length	18	24[3]
D7 centrum length	21	—
D8 centrum length	(21)	—
D9 centrum length	21	—
D10 centrum length	(19)	—
D11 centrum length	19	24[3]
D12 centrum length	(19)	—
D13 centrum length	—	24[3]
D14 centrum length	—	21[3]
S1 centrum length	—	—
S2 centrum length	18	—
S3 centrum length	19	—

CA1 centrum length	21	—
CA2 centrum length	19	—
CA3 centrum length	20	23[3]
CA4 centrum length	19	24[3]
CA5 centrum length	—	23[3]
CA6 centrum length	—	22[3]
CA7 centrum length	—	24[3]
CA8 centrum length	—	25[3]
CA9 centrum length	—	25[3]
CA10 centrum length	22	23[3]
CA11 centrum length	23	26[3]
CA12 centrum length	25	—
CA13 centrum length	(23)	—
CA14 centrum length	(21)	—
CA15 centrum length	20	—
CA16 centrum length	20	—
CA17 centrum length	21	—
CA18 centrum length	21	—
CA19 centrum length	21	—
CA20 centrum length	21	—
CA21 centrum length	23	—
CA22 centrum length	24	—
CA23 centrum length	(25)	—
CA24 centrum length	25	—
CA25 centrum length	25	—
CA26 centrum length	26	—
CA27 centrum length	26	—
CA28 centrum length	26	—
CA29 centrum length	25	—
CA30 centrum length	25	—
CA31 centrum length	24	—
CA32 centrum length	—	—
CA33 centrum length	—	—
CA34 centrum length	—	—
CA35 centrum length	—	—
CA36 centrum length	—	—
CA37 centrum length	19	—
CA40 centrum length	16[2, 3]	—
Chevron 3 length	—	50[3]
Chevron 4 length	—	46[3]
Chevron 5 length	—	32[3]
Pectoral girdle		
Scapula length	—	86
Scapular blade, minimum neck width	—	11
Scapular blade, distal width	—	24[1]

Coracoid length	—	21
Coracoid height	—	45[1]
Forelimb		
Humerus length	—	85[1]
Humeral head to apex of deltopectoral crest	—	35[1]
Radius length	—	66[1]
Ulna length (including olecranon process)	—	76[1]
Metacarpal 1 length	12[1]	18[1]
Metacarpal 2 length	19[1]	27[1]
Metacarpal 3 length	21[1]	28[1]
Metacarpal 4 length	16[1]	21[1]
Metacarpal 5 length	—	10[1]
Manual phalanx I-1 length	—	14[1]
Manual phalanx II-1 length	—	15[1]
Manual ungual II-3 length	11[1]	—
Manual phalanx III-1 length	9[1]	12[1]
Manual phalanx III-2 length	8[1]	—
Manual phalanx III-3 length	10[1]	—
Manual ungual III-4 length	(10)[1]	—
Manual phalanx IV-1 length	4[1]	—
Manual phalanx V-1 length	—	5[1,2]
Pelvic girdle		
Iliac blade length	60	—
Iliac blade height above acetabulum	32	—
Ilium, width of pubic peduncle	13	—
Ischium length	(110)	(116)
Ischium, pubic peduncle length	—	17
Ischium, iliac peduncle	—	8
Ischium, mid shaft vertical height	7	9
Pubic blade at mid length, transverse width	15	15
Pubic foot length	8[1]	10
Hind limb		
Femur length	141[1]	160
Tibia length	154	165
proximal end, anteroposterior length	27[1]	—
mid shaft, transverse width	10[1]	—
mid shaft, anteroposterior width	10[1]	—
distal end, transverse width	(11)[1]	13
Fibula length	132[1]	—
distal end, anteroposterior width	10[1]	14
Astragalus, articular surface, transverse width	24[4]	—
Astragalus, ascending process height	5[4]	—
Calcaneum, fibular articular surface, transverse width	5[4]	—
Metatarsal 1 length	(46)	—
Pedal phalanx I-1 length	18	—

Pedal phalanx II-1 length	23[1]	—
Pedal phalanx III-1 length	24[1]	—
Pedal phalanx III-2 length	16[1]	—
Pedal phalanx IV-1 length	—	13
Pedal phalanx IV-2 length	—	11
Pedal phalanx IV-3 length	—	9
Pedal phalanx IV-4 length	—	8
Pedal phalanx IV-ungual length	—	15

[1]Left side.
[2]Distalmost caudal exposed on opposite side of main slab.
[3]Exact vertebral/chevron number uncertain.
[4]From PVSJ 534, a specimen with femoral length (155 mm) that is approximately 9% longer than the holotype PVSJ 560.

3. Maturity assessment

All neural arches are attached to their respective centra and appear coossified in the holotype (PVSJ 560) and two referred specimens (PVSJ 562). Femoral lengths available in four individuals (PVSJ 534, 560-562) have a relatively narrow range of about 19 mm (~ 15%), from 141 mm in the holotype (PVSJ 560) to 160 mm in PVSJ 562. Thus, these individuals appear to have reached adult body size, corresponding to a skeletal length less than 2 m (~ 1.75 m).

4. Ischigualasto Formation: Stratigraphic summary

The Ischigualasto Formation is one of several formations in the Ischigualasto-Villa Union Basin, one of the series of small half-graben basins (*S1*) that opened in the Triassic along the southwestern margin of Pangaea (*S2*). The Ischigualasto Formation, which ranges in thickness from approximately 300-700 m, is composed predominantly of fluvial channel sandstones and floodplain overbank deposits that often show pedogenetic alteration. Sporadically throughout the section, volcanic ash beds are present, which are variously altered and reworked, several of which have been dated (see Geochronology, section 5) (*S3*).

The Ischigualasto Formation has been divided recently into four members: La Peña, Cancha de Bochas, Valle de la Luna, and Quebrada de la Sal (Fig. 4; Roman numerals I-IV to the right of the stratigraphic column) (*S4, S5*). The majority of dinosaur fossils are recorded in the lower two members (La Peña, Cancha de Bochas Members). *Eodromaeus* and *Herrerasaurus*, in addition, have been recorded in the basal portion of the third member (Valle de la Luna Member) (Fig. 4). We briefly describe these members below and divide the section into three biozones.

4a. Members

Tectonic movement along the major fault alongside the Ischigualasto Basin marked the transition from lacustrine deposition of the Los Rastros Formation and the fluvial beds of the *La Peña Member* of the Ischigualasto Formation. The interformational boundary is erosive, followed by deposition of multistory channel sandstones and conglomerates and then poorly-drained floodplain mudstones.

Floodplain deposition typically preserves disarticulated, highly weathered vertebrate bones infused with ferrous mineralization during anaerobic decay. Some degree of seasonality is indicated from plant remains (silicified roots in channel beds).

The *Cancha de Bochas Member* is characterized by a semiarid highly seasonal climate. This member is characterized by thick well-drained floodplain mudstones interbedded with mid to high-sinuosity channel sandstones. The floodplain received sporadic overflows that allowed the development of mature calcic soils (calcic vertisols, calcisols, calcic argisols) (*S4*) together with the accumulation and preservation of a time-averaged vertebrate assemblages (i.e., isolated highly weathered bone pieces together with complete articulated non-weathered skeletons), mineralized with calcium carbonate during the pedogenesis.

The *Valle de la Luna Member* is characterized by the change from calcic to argillic paleosols (argisols, gleyed vertisols), indicating an increase in humidity, although with some seasonality maintained. Amalgamated high-sinuosity channels, abandoned channels, and marsh deposits in this member preserve an array of fossil plants (i.e., tree trunks, mummified cuticles, charcoal, palynomorphs) and vertebrate fossils with hematite mineralization. Collectively, this evidence indicates the member records peak climate humidity during the time of Ischigualasto Formation deposition (from 310-650 m in a 700 m section).

The *Quebrada de la Sal Member* records a change in the fluvial system morphology to one dominated by shallow, low sinuosity channels. Although there is no fossil plant preservation, hematitic mineralization of fossils is present. The volume of volcanic ash remains high toward the top of the formation.

4b. Biozones

We summarize the distribution of 773 tetrapod fossils that we collected and mapped in the southern outcrops of the Ischigualasto Formation (Figs. 4, S1). Nineteen genera are represented; the ornithischian *Pisanosaurus* is not shown as it was found in the northern area of the formation with uncertainty as to its relative stratigraphic position (*S7, S8*). Three biozones are clear from the distribution of vertebrate remains, the boundary between the second and third corresponding to the boundary between the third and fourth members (Figs. 4, S1).

The *Scaphonyx-Exaeretodon-Herrerasaurus* biozone includes the majority of collected fossils (90%) and highest diversity (17 of 19 genera). The three namesake genera comprise 85.3% of the specimens: the rhynchosaur *Scaphonyx* (60.0%), the cynodont *Exaeretodon* (16.8%), and the basal theropod dinosaur *Herrerasaurus* (8.5%). The first two are herbivores with potentially larger populations, which might favor their preservation. The remaining 14.7% of the fauna is spread among rare amphibians (*Pelorocephalus*), synapsids, and archosauriforms including seven genera of dinosaurs. The dinosaurs include one ornithischian (*Pisanosaurus*) and six saurischians (Fig. 4). Here we use the genus *Scaphonyx*, rather than *Hyperodapedon*, because the rationale for the recent referral of the Ischigualasto rhynchosaur *Scaphonyx sanjuanensis* (*S9*) to the latter genus remains for the most part in unpublished thesis research (*S10*).

The *Exaeretodon* biozone, which includes the upper two-thirds of the Valle de la Luna Member, is characterized by the numerical dominance of specimens of the cynodont *Exaeretodon* (93.1%) and rare presence of the temnospondylid amphibian *Promastodonsaurus* (1.4%), the crurotarsans *Saurosuchus* (1.4%) and *Aetosauroides* (2.7%), and the archosauriform *Proterochampsa* (1.4%).

The *Jachaleria* biozone is almost devoid of vertebrate fossils. Only two specimens have been recovered, such that the interval is defined more on the absence of fossils. A single bone of the dicynodont *Jachaleria* and a couple of bones tentatively assigned to a nondinosaurian archosaur constitute the vertebrate record for the Quebrada de la Sal Member.

The vertebrate fauna recorded from the Ischigualasto Formation shows two principal transitions that divide the section into three biozones. The first is the extinction of the rynchosaur *Scaphonyx* and the simultaneous disappearance of dinosaurs and most of the therapsid genera. The persistence of relatively small-bodied cynodonts (*Exaeretodon*) and basal archosauromorphs (*Proterochampsa, Aetosauroides*) and the absence of the larger-bodied *Scaphonyx* and *Herrerasaurus* suggests that this faunal shift captures a regional extinction event rather than taphonomic bias in the preservation of specimens. The end of the range of *Scaphonyx* previously was thought to be linked to the demise of the *Dicroidium* flora (*S10*). It appears more likely to be related to increasing humidity. The extinction of *Herrerasaurus*, the most common predator in the fauna, may have been related to its reliance on *Scaphonynx*, the most common herbivore.

The second marked faunal shift is the disappearance of the cynodont *Exaeretodon* and the appearance of a mid-sized dicynodont *Jachaleria* at the beginning of the *Jachaleria* biozone. Tectonic events affecting sedimentation rate may have had a greater effect than climatological changes , although the latter may have limited the potential for preservation of vertebrate remains. Vertebrate remains in the lower portion of the overlying Los Colorados Formation (Norian) follow the same pattern, with scarce dyconodont material and no remains of the formerly abundant cynodont *Exaeretodon.*

In the *Scaphonyx-Exaeretodon-Herrerasaurus* biozone, which is by far the best represented and diverse, dinosaurs encompass approximately 11% of all finds. This high number is significant, given that the fauna is dominated by undoubted nondinosaurian herbivores (*Scaphonyx, Exaeretodon*); the most numerous dinosaurs are herrerasaurids (*Herrerasaurus*, *Sanjuansaurus*), undoubted carnivores. *Eodromaeus* is also a carnivore. Herrerasaurids comprise 72% of all recovered terrestrial carnivores. *Eoraptor* (*S11*), *Panphagia* (*S12*) and a fragmentary and possibly new basal sauropodomorph, *Chromogisaurus* (*S13*), are probably herbivores or omnivores rather than carnivores. Along with *Pisanosaurus*, these dinosaurs are rare compared to the undoubted herbivores in the biozone (1-2%), although they represent all of the small herbivores. In terms of diversity, dinosaurs (33%) along with therapsids (33%), are the most diverse at the generic level, followed by crurotarsan archosaurs (22%) and basal archosauromorphs (11%).

5. Ischigualasto Formation: $^{40}Ar/^{39}Ar$ geochronology

5a. Age estimate near the top of the formation

Sixteen feldspar grains were analyzed by total fusion, yielding a coherent population of eight grains of low Ca/K (2.0-4.0) plagioclase with a nominal (see following section for definition) weighted mean age of 223.84 ± 0.88 Ma (Table S2, date 1). Eight additional grains, which are interpreted as xenocrysts, yielded nominal ages ranging from 227-774 Ma. Six of these are sanidine or anorthoclase based on Ca/K < 0.2.

Stepwise heating in 4 or 5 steps with a defocused laser beam was attempted individually on an additional 24 crystals. Most failed to yield useful results due to very small ion beams or proved to be xenocrysts. Five yielded nominal plateau ages from 218 ± 7 Ma to 226 ± 6 Ma. Their nominal weighted mean age is 223.10 ± 2.20 Ma, indistinguishable from the younger mode of the total fusion results (Table S2). Because single-crystal age spectra do not indicate partial ^{40}Ar loss, results from the two types of experiments are combined to yield a pooled nominal age of 223.79 ± 0.87 Ma.

Large uncertainties have been noted in the ^{40}K decay constants used to calculate nominal ages (*S14*). More accurate calibration is provided by the results of Kuiper et al. (*S15*) and a more recent calibration (*S16*). In Table S2 we compare the results of this calibration with the nominal age. We also include the ^{40}Ar/^{39}Ar age (227.8 ± 0.3 Ma) previously reported for the Herr Toba bentonite, which was originally reported as 227.8 Ma relative to an age of 27.84 Ma for the FCs standard (*S3*).

We prefer to use the ages based on the Renne et al. calibration (*S16*), as these are most appropriate for comparison with ages determined by other methods and the timescale we have employed. Thus the age and error assigned to ISCH-6-611 is 225.9 ± 0.9 Ma (Table S2).

Table S2. Early and late ^{40}Ar/^{39}Ar ages (from 20 m and 630 m in a section of approximately 700 m across La Gallinita) (Fig. 4) from the Ischigualasto Formation, with the absolute age and error calculated by three methods.

No.	Sample	Section level (700 m)	Nominal[1] (Ma)	Kuiper[2] (Ma)	Renne[3] (Ma) (preferred age estimate)
1	ISCH-6-611	630 m	223.8 ± 0.9	225.3 ± 0.9	225.9 ± 0.9
2	Herr Toba	20 m	229.2 ± 0.3	230.8 ± 0.4	231.4 ± 0.3

[1]Nominal age is based on an age of 28.02 Ma for FCs (*S16*) and ^{40}K decay constants (*S21*) and ignores uncertainties associated with standards and decay constants.

[2]Kuiper age is based on an age of 28.201 Ma for FCs and ^{40}K decay constants (*S14*), and includes systematic errors in the ^{40}K decay constants and isotopic data for the FCs standard.

[3]Renne age based on a recent calibration (*S16*), which uses a a compilation of ^{40}K activity data, isotope data for the standard, and intercalibration with the ^{238}U/^{206}Pb system. The uncertainty includes contributions from all known sources of error.

5b. Methods for age estimation

Feldspars in the 0.3 to 0.5 mm size fractions were separated from sample ISCH-6-611 using standard techniques, then irradiated in the cadmium-lined in-core irradiation tube (CLICIT) facility at the Oregon State University TRIGA research reactor. Samples

were irradiated in wells in an Al disk (*S17*) along with crystals of the Fish Canyon sanidine (FCs) standard. *J*-values were determined from individual analysis of 5 to 8 FCs crystals from each of six wells bracketing the samples, and the arithmetic mean and standard deviation (0.0026688 ± 0.0000826) of values for these six positions was used for age calculations (Tables S3, S4).

Single crystals were degassed with a CO_2 laser either by total fusion or by step-wise laser power increase. Extracted gas was purified by passive gettering and exposure to a cryocooler at ~ -130 °C for 180 s before admission to the mass spectrometer. Mass spectrometry followed methods described by (*S16*). Procedural blanks were measured between every three unknowns and were similar to values reported previously (*S14*). Mass discrimination (1.0063 ± 0.0015 and 1.0063 ± 0.0016 per amu for the total fusion and step-heating analyses, respectively) was determined from analyses of 50 aliquots from an automated on-line air pipette system, regularly interspersed with the unknowns and standards, and the discrimination correction was applied as a power law function (*S18*).

Interfering Ar isotopes from Ca, K and Cl were corrected for production ratios (*S19, S20*). Nominal ages were calculated using an age of 28.02 Ma for FCs (*S17*) and constants from the literature (*S21*). Uncertainties on nominal ages do not include contributions from the age of the standard or the decay constants.

Table S3. Constants used in age estimation

Constants used		Reference
Atmospheric argon ratios		
$(^{40}Ar/^{36}Ar)_A$	296.0±0.74	Nier (1950)
$(^{40}Ar/^{38}Ar)_A$	0.1880±0.0001	Nier (1950)
Interfering isotope production ratios		
$(^{40}Ar/^{39}Ar)_K$	(7.30±0.92)E-04	Renne et al. (2005)
$(^{38}Ar/^{39}Ar)_K$	(1.22±0.00)E-02	Renne et al. (2005)
$(^{37}Ar/^{39}Ar)_K$	(2.24±0.16)E-04	Renne et al. (2005)
$(^{39}Ar/^{37}Ar)_{Ca}$	(6.95±0.09)E-04	Renne et al. (2005)
$(^{38}Ar/^{37}Ar)_{Ca}$	(1.96±0.08)E-05	Renne et al. (2005)
$(^{36}Ar/^{37}Ar)_{Ca}$	(2.65±0.02)E-04	Renne et al. (2005)
$(^{36}Cl/^{38}Cl)_{Cl}$	263±2	Renne et al. (2008)
Decay constants		
$^{40}K\ \lambda_{\varepsilon}$	(5.81±0.00)E-11 a^{-1}	Steiger & Jäger (1977)
$^{40}K\ \lambda_{\beta}$	(4.962±0.000)E-10 a^{-1}	Steiger & Jäger (1977)
^{39}Ar	(2.58±0.03)E-03 a^{-1}	Stoenner et al. (1969)
^{37}Ar	(5.4300±0.0063)E-02 a^{-1}	Renne & Norman (2001)
$^{36}Cl\ \lambda_{\beta}$	(2.35±0.02)E-06 a^{-1}	ENSDF

Table S4. Source of J and use of J adjustment values.

Run ID	Laser (W)[a]	^{40}Ar (moles)	^{40}Ar (nA)[c]	σ (nA)[c]	^{39}Ar (nA)[c]	σ (nA)[c]	^{38}Ar (nA)[c]	σ (nA)[c]	^{37}Ar (nA)[c]	σ (nA)[c]	^{36}Ar (nA)[c]	σ (nA)[c]	^{40}Ar* / ^{39}Ar$_K$ ([d])	σ	% ^{40}Ar* ([e])	Age (Ma)[f]	σ (Ma)[g]
Total Fusion Analyses																	
D=1.00625±0.00147[b]																	
33022-05	**7.0**	**1.50E-13**	**0.64439**	**0.00180**	**0.127087**	**0.000264**	**0.001605**	**0.000029**	**0.23629**	**0.00293**	**0.000140**	**0.000025**	**4.896**	**0.061**	**96.4**	**221.55**	**2.59**
33022-12	**7.0**	**1.96E-13**	**0.84528**	**0.00162**	**0.169865**	**0.000291**	**0.002100**	**0.000034**	**0.23319**	**0.00296**	**0.000110**	**0.000024**	**4.897**	**0.045**	**98.3**	**221.59**	**1.90**
33022-06	**7.0**	**2.07E-13**	**0.88958**	**0.00192**	**0.179184**	**0.000191**	**0.002239**	**0.000031**	**0.24543**	**0.00295**	**0.000087**	**0.000024**	**4.932**	**0.043**	**99.3**	**223.08**	**1.80**
33022-13	**7.0**	**2.20E-13**	**0.94884**	**0.00166**	**0.175620**	**0.000239**	**0.002143**	**0.000034**	**0.29856**	**0.00294**	**0.000360**	**0.000024**	**4.935**	**0.043**	**91.2**	**223.21**	**1.81**
33022-14	**7.0**	**3.14E-13**	**1.35084**	**0.00212**	**0.271082**	**0.000478**	**0.003386**	**0.000035**	**0.39755**	**0.00302**	**0.000132**	**0.000024**	**4.959**	**0.029**	**99.4**	**224.23**	**1.25**
33022-11	**7.0**	**2.91E-13**	**1.25170**	**0.00172**	**0.249040**	**0.000402**	**0.003051**	**0.000031**	**0.31105**	**0.00294**	**0.000139**	**0.000024**	**4.963**	**0.031**	**98.7**	**224.41**	**1.31**
33022-10	**7.0**	**2.39E-13**	**1.02916**	**0.00162**	**0.198159**	**0.000282**	**0.002474**	**0.000030**	**0.23392**	**0.00294**	**0.000211**	**0.000024**	**4.975**	**0.039**	**95.7**	**224.92**	**1.64**
33022-15	**7.0**	**1.58E-13**	**0.67862**	**0.00178**	**0.134652**	**0.000291**	**0.001599**	**0.000029**	**0.19681**	**0.00292**	**0.000071**	**0.000024**	**5.004**	**0.055**	**99.2**	**226.14**	**2.34**
33022-09	7.0	4.25E-14	0.18300	0.00157	0.032566	0.000170	0.000433	0.000024	0.00061	0.00284	0.000064	0.000023	5.036	0.212	89.6	**227.50**	8.95
33022-16	7.0	3.38E-13	1.45576	0.00212	0.275028	0.000450	0.003465	0.000035	0.26053	0.00294	0.000180	0.000024	5.176	0.029	97.7	**233.45**	1.23
33022-07	7.0	1.80E-13	0.77352	0.00179	0.128799	0.000247	0.001546	0.000030	0.18118	0.00291	0.000069	0.000024	5.962	0.058	99.2	**266.37**	2.40
33022-01	7.2	8.27E-14	0.35580	0.00165	0.038197	0.000170	0.000474	0.000024	0.00374	0.00283	0.000110	0.000023	8.475	0.184	91.0	**367.87**	7.21
33022-04	7.0	7.27E-12	31.24442	0.01707	3.562936	0.002206	0.042882	0.000102	0.01144	0.00287	0.000179	0.000031	8.754	0.015	99.8	**378.79**	0.59
33022-02	7.0	5.45E-12	23.42253	0.01110	2.622353	0.002106	0.031777	0.000092	0.13590	0.00289	0.000179	0.000032	8.915	0.016	99.8	**385.07**	0.62
33022-03	7.0	3.74E-12	16.09864	0.00903	1.799032	0.001208	0.021735	0.000071	0.16833	0.00288	0.000182	0.000030	8.926	0.016	99.7	**385.48**	0.63
33022-08	7.0	1.23E-13	0.52946	0.00166	0.023543	0.000170	0.000306	0.000023	0.00218	0.00284	0.000194	0.000023	20.064	0.336	89.2	**773.68**	10.49
Wtd. Mean													**4.950**	**0.014**		**223.84**	**0.88**
Step Heating Analyses																	
D=1.00633±0.00163[b]																	
33022-26A	**0.1**	**6.15E-15**	**0.02648**	**0.00095**	**0.004144**	**0.000065**	**0.000025**	**0.000020**	**0.00370**	**0.00042**	**0.000019**	**0.000022**	**5.092**	**1.615**	**79.7**	**229.88**	**68.45**
33022-26B	**0.3**	**1.52E-14**	**0.06548**	**0.00098**	**0.013252**	**0.000070**	**0.000125**	**0.000021**	**0.01539**	**0.00049**	**-0.000005**	**0.000021**	**5.138**	**0.471**	**103.9**	**231.84**	**19.93**
33022-26C	**0.5**	**6.76E-14**	**0.29127**	**0.00111**	**0.057651**	**0.000197**	**0.000745**	**0.000023**	**0.07494**	**0.00103**	**0.000041**	**0.000021**	**4.949**	**0.110**	**97.9**	**223.82**	**4.68**
33022-26D	**0.7**	**2.36E-14**	**0.10174**	**0.00096**	**0.020032**	**0.000066**	**0.000261**	**0.000020**	**0.02427**	**0.00049**	**0.000011**	**0.000021**	**5.009**	**0.311**	**98.6**	**226.37**	**13.21**
33022-26E	**0.9**	**3.11E-14**	**0.13378**	**0.00095**	**0.026273**	**0.000086**	**0.000280**	**0.000021**	**0.03143**	**0.00058**	**0.000021**	**0.000023**	**4.949**	**0.260**	**97.1**	**223.83**	**11.07**
Wtd. Mean													**4.963**	**0.094**		**224.40**	**4.01**
33022-35A	**0.1**	**3.05E-15**	**0.01311**	**0.00094**	**0.001731**	**0.000057**	**0.000016**	**0.000020**	**0.00277**	**0.00040**	**0.000010**	**0.000021**	**6.064**	**3.590**	**80.0**	**270.61**	**148.78**
33022-35B	**0.3**	**3.32E-15**	**0.01426**	**0.00094**	**0.002415**	**0.000056**	**0.000034**	**0.000019**	**0.00507**	**0.00041**	**0.000005**	**0.000021**	**5.438**	**2.570**	**92.0**	**244.48**	**108.07**
33022-35C	**0.5**	**5.18E-14**	**0.22311**	**0.00137**	**0.044046**	**0.000197**	**0.000520**	**0.000023**	**0.09895**	**0.00076**	**0.000052**	**0.000023**	**4.903**	**0.159**	**96.7**	**221.84**	**6.75**

33022-35D	**0.7**	**2.88E-15**	**0.01241**	**0.00095**	**0.002211**	**0.000056**	**0.000020**	**0.000019**	**0.00448**	**0.00046**	**0.000003**	**0.000021**	**5.317**	**2.804**	**94.6**	**239.40**	**118.24**
Wtd. Mean													**4.908**	**0.158**		**222.08**	**6.72**
33022-41A	**0.1**	**9.96E-15**	**0.04285**	**0.00094**	**0.003612**	**0.000056**	**0.000049**	**0.000019**	**0.00029**	**0.00041**	**0.000069**	**0.000024**	**6.200**	**1.973**	**52.3**	**276.26**	**81.51**
33022-41B	**0.3**	**8.80E-15**	**0.03786**	**0.00094**	**0.007277**	**0.000057**	**0.000081**	**0.000020**	**-0.00017**	**0.00041**	**0.000002**	**0.000021**	**5.101**	**0.848**	**98.1**	**230.24**	**35.93**
33022-41C	**0.5**	**4.89E-14**	**0.21039**	**0.00104**	**0.042022**	**0.000097**	**0.000549**	**0.000023**	**0.00029**	**0.00043**	**0.000029**	**0.000023**	**4.801**	**0.163**	**95.9**	**217.52**	**6.96**
33022-41D	**0.7**	**8.35E-15**	**0.03593**	**0.00094**	**0.006390**	**0.000057**	**0.000077**	**0.000020**	**-0.00026**	**0.00044**	**0.000023**	**0.000021**	**4.570**	**0.966**	**81.3**	**207.62**	**41.46**
Wtd. Mean													**4.814**	**0.158**		**218.07**	**6.72**
33022-43A	**0.1**	**2.11E-14**	**0.09077**	**0.00100**	**0.001332**	**0.000062**	**0.000080**	**0.000021**	**0.00082**	**0.00040**	**0.000279**	**0.000024**	**6.413**	**5.496**	**9.4**	**285.02**	**225.97**
33022-43B	**0.3**	**8.32E-15**	**0.03578**	**0.00094**	**0.006869**	**0.000059**	**0.000039**	**0.000019**	**0.01070**	**0.00044**	**0.000004**	**0.000021**	**5.177**	**0.899**	**99.3**	**233.50**	**38.03**
33022-43C	**0.5**	**3.33E-14**	**0.14341**	**0.00098**	**0.027935**	**0.000098**	**0.000345**	**0.000020**	**0.05079**	**0.00063**	**0.000017**	**0.000021**	**5.097**	**0.223**	**99.2**	**230.10**	**9.46**
33022-43D	**0.7**	**3.94E-14**	**0.16954**	**0.00097**	**0.032767**	**0.000091**	**0.000423**	**0.000023**	**0.05965**	**0.00068**	**0.000047**	**0.000023**	**4.900**	**0.213**	**94.6**	**221.73**	**9.09**
Wtd. Mean													**5.001**	**0.152**		**226.00**	**6.46**
33022-44A	**0.1**	**2.81E-15**	**0.01210**	**0.00094**	**0.001322**	**0.000059**	**0.000013**	**0.000020**	**0.00053**	**0.00040**	**0.000013**	**0.000021**	**6.199**	**4.676**	**67.7**	**276.20**	**193.19**
33022-44B	**0.3**	**7.26E-15**	**0.03124**	**0.00094**	**0.006084**	**0.000062**	**0.000059**	**0.000020**	**0.00865**	**0.00045**	**0.000003**	**0.000021**	**5.109**	**1.012**	**99.4**	**230.59**	**42.87**
33022-44C	**0.5**	**2.24E-14**	**0.09662**	**0.00095**	**0.019012**	**0.000078**	**0.000234**	**0.000020**	**0.02874**	**0.00057**	**0.000021**	**0.000023**	**4.886**	**0.367**	**96.1**	**221.13**	**15.64**
33022-44D	**0.7**	**8.49E-14**	**0.36585**	**0.00101**	**0.073580**	**0.000121**	**0.000893**	**0.000023**	**0.11017**	**0.00077**	**0.000041**	**0.000021**	**4.931**	**0.085**	**99.1**	**223.05**	**3.63**
Wtd. Mean														**4.930**	**0.1**	**223.02**	**3.53**

Notes

Data shown in **boldface** are those used in age calculations.

[a]Laser power output in watts.

[b]Mass discrimination per atomic mass unit (dalton), applied as a power law correction

[c]Amplified ion beam current measured on a single analog electron multiplier; corrected for mass discrimination, background, and radioactive decay.

[d]Ratio of radiogenic ^{40}Ar to reactor-produced ^{39}Ar by neutron capture on ^{39}K.

[e]Percentage of ^{40}Ar that is radiogenic rather than atmospheric or reactor-produced.

[f]Nominal age in millions of years based on Steiger & Jäger (1977) constants and standard calibration of Renne et al. (1998).

[g]Age uncertainty neglecting contributions from ^{40}K decay constants or age of the standard.

5c. Previous age estimates

In addition to the two dates discussed above for the Ischigualasto Formation, two other dates have been reported in the literature. The first comes from basalt flows in the Los Rastros Formation just below the contact with the overlying Ischigualasto Formation (*S5*). The reported age (229.0 ± 5 Ma) is approximately 2 million years older than the Herr Toba, which comes from a level about 20 m above the base of the Ischigualasto Formation. Without knowing more information about this sample and the details of the dating protocol, we can only say that its age (using the preferred decay constants indicated above) would likely exceed 231 ± 5 Ma, and thus would be consistent with the date just above it at the base of the Ischigualasto section (231.4 ± 0.3 Ma).

The second date (217.0 ± 1.7 Ma) is based on an altered ash and comes from a complete section of less certain correlation at the eastern extremity of the outcrop of the Ischigualasto Formation (*S5*). It was first reported in an unpublished thesis (*S22*). In addition to uncertainty in its stratigraphic location, two age estimates were originally reported and the methodology used to arrive at these estimates has yet to be detailed. We therefore regard this age as unreliable.

6. Phylogenetic analysis

6a. Parsimony analysis

The phylogenetic analysis focuses on the most completely known taxa close to the base of the dinosaurian radiation (Fig. 3), with details to be presented elsewhere (Sereno, unpublished data). The aim is to isolate the most important characters and taxa relevant to this problem rather than attempt to position all more poorly known genera within a single phylogenetic scheme. The five suprageneric taxa used in this analysis are represented by a consensus score based on specific exemplars (Table S5). In this way, we maintained focus on the problem at hand, while (1) maintaining species-level coding, (2) combining information on important subclades known from less complete genera, such as Lagerpetonidae and Silesauridae, and (3) representing very diverse subclades that are widely regarded as monophyletic, such as Genasauria or Sauropodiformes without being overwhelmed by superfluous character data in support of their monophyly.

Three successively more remote outgroups were used (Silesauridae*,* *Marasuchus*, Lagerpetonidae), based on an emerging consensus regarding their position relative to Dinosauria (*S23*). Ingroups include three suprageneric taxa (Heterodontosauridae, Genasauria, Sauropodiformes) and 12 species. One or more of the authors have examined material pertaining to species exemplars within these taxa, with the exception of the Silesauridae (Table S5). With this sampling of ingroups, the phylogenetic position of all of the best known basal dinosaurs can be effectively evaluated.

Table S5. Taxa, references and specimens used for outgroups and ingroups in the phylogenetic analysis.

Taxa	No.	Terminal Taxon	Exemplars for Supraspecific Terminal Taxa
Outgroups	**1**	LAGERPETONIDAE	*Lagerpeton chanarensis* *Dromomeron romeri*
	2	*Marasuchus lilloensis*	
	3	SILESAURIDAE	*Silesaurus opolensis* *Asilisaurus kongwe*
Ingroups	**1**	HETERODONTOSAURIDAE	*Heterodontosaurus tucki* *Tianyulong confuciusi*
	2	*Lesothosaurus diagnosticus*	
	3	GENASAURIA	*Scutellosaurus lawleri* *Hypsilophodon foxii* *Psittacosaurus mongoliensis*
	4	*Eoraptor lunensis*	
	5	*Panphagia protos*	
	6	*Saturnalia tupiniquim*	
	7	SAUROPODIFORMES	*Massospondylus carinatus* *Plateosaurus engelhardti*
	8	*Eodromaeus murphi*	
	9	*Herrerasaurus ischigualastensis*	
	10	*Staurikosaurus pricei*	
	11	*Tawa hallae*	
	12	*Coelophysis bauri*	
	13	*Syntarsus rhodesiensis*	
	14	*Syntarsus kayentakatae*	
	15	*Dilophosaurus wetherilli*	
	16	*Ceratosaurus nasicornis*	

6b. Character list and matrix

139 characters were scored in 16 basal dinosaurian taxa, using three successive dinosaurian outgroups (Table S5). A hypothetical ancestral dinosauromorph was added to the outgroups, polarizing a few additional characters that are currently unknown in available basal dinosauromorphs but present among more distant outgroups. The list is a revision and expansion of character data in a previous analysis of basal relationships within Dinosauria (*S24*, suppl. info. matrix 1).

Some of the characters in the 1999 analysis were eliminated because they were uninformative in the original analysis, others because they were regarded as too

ambiguous or overlapping in the light recent methods for character formulation (*S27-S29*); others were eliminated as uninformative after restriction of terminal taxa to basal nodes within Dinosauria and removal of the most poorly known taxa (*Pisanosaurus, Chindesaurus*). Eliminated characters include 1-5, 9, 11-14,17, 54, 56, 57, 63, 68, 75, 77, 78-82, 85-87, 89, 105, 106, 111, 113, 123, 124, 130, 133, 136, 137, 138, 140, 145, 146, and 158. In all 119 characters in the list and matrix below are from the original set of 146.

Characters were added from independent analyses in the same study (*S24*; Prosauropoda, Ceratosauria) and recent analyses of Tykoski (2005) (*S31*), Langer and Benton (2006) (*S25*), Ezcurra and Novas (2007) (*S33*), Nesbitt et al. (2009) (*S26*), and Ezcurra (2010) (*S13*) (see comparative discussion in section 6c below).

There are 11 multistate characters (48, **59**, **76**, **78**, **85**, 88, 98, 112, 120, 123, **130**), 5 of which have successively inclusive states and are ordered (bold). Former character numbers from data matrices in Sereno (1999, suppl. info.) (*S24*) are given. Characters in red are added from other matrices in *S24* or other sources as cited. A comparative assessment of the character data used to assess dinosaur origins in the many cladistic analyses that have considered the problem is needed but is beyond the scope of this study (Sereno, unpublished data).

Character List

Cranium

1. Skull length relative to 3 times posterior skull height: less (0); more (1). (Sereno, 1999, matrix 7, character 33) (correlated characters: increased tooth number, length of antorbital fossa, fenestra, etc.)
2. External naris, size: small, set within tapered snout end (0); large, expanded narial margin (1). (formerly 73)
3. Subnarial foramen: absent (0); present (1). (formerly 62)
4. Antorbital fossa, ventral margin, rounded laterally-protruding rim: absent (0); present (1). (= “alveolar ridge” sensu Rowe, 1987; Sereno, 1999; matrix 7, character 44)
5. Antorbital fossa and fenestra, size relative to snout (lateral view): large, near maxilla-nasal suture (0); small, separated from maxilla-nasal suture (1). (formerly 29)
6. Premaxilla, medial premaxillary foramen: absent (0); present (1). (formerly 109)
7. Premaxilla, posterolateral process, length: short (0); long, extending at least to the posterior end of the external naris, subequal to premaxillary body in length (1). (formerly 27; Tykoski, 2005)
8. Premaxilla, posterolateral process, articulation: lateral aspect of snout (0); dorsal aspect of maxillary anteromedial process (1). (formerly 76)
9. Premaxilla-maxilla, diastema: absent (0); present (1). (formerly 55)
10. Premaxilla, posteroventral flange (backing dorsal portion of arched diastema): absent (0); present (1). (Rauhut, 2003; Tykoski, 2005). (= “forked” premaxillary posterolateral process)
11. Premaxilla-nasal, suture, form: V-shaped (0); W-shaped (1). (formerly 108)
12. Premaxilla-maxilla, alveolar suture: present (0); absent (1). (Sereno, 1999; matrix 7, character 35) (correlated characters: arched premaxilla-maxilla diastema, “kinetic” premaxilla)
13. Premaxilla, palatal process: present (0); absent (1). (Tykoski, 2005).
14. Premaxilla, palate, depth: as deep as broad (0); broader than deep (1). (formerly 26)
15. Maxilla, anteriormost alveolar margin, form (lateral view): approximately horizontal, maxillary tooth 1 vertical (0); anterodorsally upturned, maxillary tooth 1 inclined anteroventrally at about 45° from the vertical (1). (Rowe, 1989; Tykoski, 2005)
16. Maxilla, buccal emargination (cheek): absent (0); present (1). (formerly 52)
17. Maxilla, border of external nares: absent (0); present (1). (formerly 74, character state order reversed)
18. Maxilla, promaxillary fenestra and antrum: absent (0); present (1). (formerly 112)
19. Nasal, posterolateral process: absent (0); present (1). (formerly 110)

20. Lacrimal, ventral half of ventral process, subtriangular flange medial to antorbital fossa (exposed in lateral view): absent (0); present (1). (new character)
21. Lacrimal, mid section of ventral process, lateral antorbital fossa wall (lateral view): straight border (0); crescentic flange dividing dorsal and ventral exposures of the medial antorbital wall (1). (formerly 114)
22. Jugal, posterior process, quadratojugal articulation, form: subtriangular (0); deeply forked (1). (formerly 64)
23. Postorbital, participation in supratemporal fossa: present (0); absent (1). (Sereno, 1999; matrix 7, character 54)
24. Squamosal, ventral process, shape: transversely compressed flange (0); slender prong 3 or more times basal width (1). (Sereno, 1999, matrix 5, character 5)
25. Squamosal, anterior process, orientation (lateral view): anterior (0); anterodorsal inclined 30° or more (1). (formerly 115)
26. Palpebral: absent (0); present (1). (formerly 30)
27. Palatine, anterior process, shape: triangular, tapering distally (1); lobe-shaped with basal constriction (1). (formerly 116)
28. Exoccipital-opisthotic, process forming lateral margin of basal tubera: absent (0); present (1). (formerly 117)
29. Laterosphenoid-frontal, contact: present (0); absent (head contacts postorbital only) (1). (formerly 118)
30. Basisphenoid fontanelle: present (0); absent (1). (formerly 119)

Lower Jaw

31. Intramandibular joint: absent (0); present (1). (formerly 88)
32. Intramandibular joint, polarity of articulation: (0) splenial convex, angular concave (0); splenial concave, angular convex (1). (formerly 103)
33. External mandibular fenestra, anteroposterior diameter relative to the maximum depth of dentary ramus: more (0); subequal or less (1). (formerly 24)
34. Predentary: absent (0); present (1). (formerly 31)
35. Dentary symphysis, form: transversely narrow, V-shaped (0); spout-shaped (1). (formerly 32)
36. Dentary, coronoid process: absent (0); present (1). (formerly 23)
37. Dentary, coronoid process, length relative to depth of the dentary at mid length: approximately 35% or less (0); 50% or more (1). (formerly 53)
38. Prearticular-angular/splenial foramen: absent (0); present (1). (formerly 120)

Dentition

39. Premaxillary tooth number: 4 (0); 3 (1); 5 or 6 (2). (formerly 19)
40. Premaxillary tooth 1, position: adjacent to midline (0); inset posteriorly (distally) the width of one or more crowns (1). (formerly 25)
41. Premaxillary teeth, position of posteriormost tooth relative to external naris: ventral (0), or anterior (1). (Sereno, 1999; matrix 7, character 36)
42. Maxillary/dentary teeth, position of largest tooth in tooth row: anterior (mesial) end (0), or center (1). (formerly 22)
43. Maxillary/dentary crowns, shape: recurved (0); subtriangular (1); lanceolate (2). (formerly 20)
44. Maxillary/dentary crowns, marginal ornamentation, form: serrations (0); denticles (1). (formerly 21)
45. Dentary tooth 1, position: terminal (0); inset (1). (Sereno, 1999, matrix 5, character 6)
46. Pterygoid teeth: present (0); absent (1). (formerly 107)

Axial Column

47. Axis, intercentrum, width relative to maximum width of axial centrum: less (0); more (1). (formerly 96)
48. Axis, neural canal diameter relative to 25% centrum diameter: more (0); less (1). (formerly 122)
49. Cervical centra (postatlantal), rimmed pleurocoels in some or all: absent (0); present (1). (formerly 121)
50. Cervical centra (postatlantal), posterior articular surface: flat or shallow concavity (0); deeply cupped (“opisthocoelous”) (1). (formerly 125)
51. Mid cervical (C3-C6) centra, length relative to centrum height: less than 3 (0); 3 (1); more than 4 (2). (Sereno, 1999; matrix 7, character 45)
52. Mid or posterior cervicals, epipophyses: absent or low crest (0); prong-shaped, overhanging process (1). (formerly 65, 89)

53. Posterior cervical and dorsal vertebrae, transverse process shape: subrectangular (0); subtriangular (1). (Sereno, 1999; matrix 7, character 56)
54. Dorsal centra, length relative to height: subequal (0); more than 2.5 times (1). (Sereno, 1999; matrix 7, character 48)
55. Dorsal vertebrae, hyposphene-hypantrum articulation: absent (0); present (1). (formerly 66)
56. Sacrals, shape (dorsal view): subrectangular (0); subtriangular (1). (Sereno, 1999; matrix 7, character 57)
57. Sacrals, transverse processes, relation: separate (0); joined (1). (Sereno, 1999; matrix 7, character 58)
58. Dorsosacral 1 (transverse process contacting preacetabular process): absent (0); present (1). (formerly 6)
59. Caudosacrals 1 (transverse process contacting postacetabular process): absent (0); present (1). (formerly 127)
60. Caudosacrals 2 (transverse process contacting postacetabular process): absent (0); present (1). (formerly 127)
61. Caudosacral ribs, attachment on postacetabular process: ventral margin (0); inclined from ventral margin to posterodorsal corner (1). (formerly 128)
62. Distal caudal centra, length relative to centrum height: 3 to 5 times (0); 7 times (1). (Sereno, 1999; matrix 7, character 59)
63. Distal caudals, prezygapophyses, length: short, little overlap (0); elongate, overlap 25% or more of preceding centrum (1). (formerly 97)
64. Mid cervical ribs, length relative to centrum length: less (0); more (overlapping) (1). (formerly 67)
65. Sternal plates (paired, ossified): absent (0); present (1). (formerly 7)
66. Gastralia: present (0); absent (1). (formerly 51)
67. Epaxial tendons (ossified): absent (0); present (1). (formerly 50)

Pectoral Girdle

68. Scapula, blade, length relative to distal width: less than 3 times (0); more than 3 times (1). (formerly 98)

Forelimb

69. Humerus, deltopectoral crest, length relative to humeral length: 30% or less (0); 35-44% (1); 45% or more (2). (formerly 8)
70. Manus, length (longest digit) relative to humerus + radius: 20-30% (0); approximately 40% (1); 50-70% (2). (formerly 69)
71. Manus, digits and metacarpals, longest: digit III, metacarpal 3 (0); digit II, metacarpal 2 (1). (formerly 131)
72. Manus digit V: present (0); absent (1). (formerly 132)
73. Metacarpals 1-3, base, flat intermetacarpal articular facets: absent (0); present (1). (formerly 91)
74. Metacarpals 1-3, distal end, extensor depressions: absent (0); present (1). (formerly 92)
75. Metacarpals 4 and 5, mid shaft diameter relative to metacarpal 2 or 3: subequal (0); less than 50% (1). (formerly 100)
76. Manus digit I phalanx 1, rotation of axis through distal condyles: no rotation or slight ventrolateral rotation (0); rotated 45° ventromedially (1); rotated 60° ventromedially (2). (Sereno, 1999, matrix 5, character 14)
77. Manus digit I phalanx 1, length relative to metacarpal 1: shorter (0); subequal to or longer (1). (formerly 70)
78. Manus digits I-III and penultimate phalanx (digits II, III), length; and ungual (digits I-III), form: shorter or subequal to preceding phalanx, moderately recurved unguals (0); longer than preceding phalanx, trenchant unguals (1). (formerly 99)

Pelvic Girdle

79. Ilium, preacetabular process, shape: tab-shaped (0); strap-shaped (1); subtriangular (2); semicircular (3). (formerly 33)
80. Ilium, preacetabular process, position of distal end relative to the distal end of pubic peduncle: posterior (0); anterior (1). (formerly 34)
81. Ilium, preacetabular process, attachment scar: absent (0); present (1). (Sereno, 1999, matrix 5, character 17)
82. Ilium, ischial peduncle, axis of process: ventrally directed (0); ventrolaterally directed (1). (formerly 61)

83. Ilium, ventral acetabular flange: present (0); absent (1). (formerly 83)
84. Ilium, supraacetabular crest, form: shelflike, gently transversely arched (0); pendant, overhanging femoral head (1). (Sereno, 1999; matrix 7, character 3)
85. Ilium, postacetabular process, posterior margin, shape: convex (0); concave (1). (Sereno, 1999; matrix 7, character 5)
86. Ilium, postacetabular process, lateral attachment scar, form: subtle (0); pronounced rim (1). (Rowe, 1989; Sereno, 1999; matrix 7, character 60)
87. Ilium, postacetabular process, brevis fossa: absent (0); present (1). (formerly 10)
88. Ilium, bevis fossa, shape and orientation: broad laterally-open depression (0); shallow groove or absent (1); arched ventrally-opening ovate or parallel-sided depression (2); arched ventrally-opening posteriorly-expanding to a width approximately 50% of its length (3). (formerly, 93; Sereno, 1999; matrix 7, character 4)
89. Ischium, obturator process: absent (0); present (1). (formerly 94)
90. Ischium, mid shaft, cross-sectional shape: oval or elliptical (0); subtriangular (1). (Sereno, 1999, matrix 5, character 17)
91. Ischium, mid shaft, variation in transverse width: uniform or gently decreasing distally (0); expanding distally (1). (formerly 42)
92. Ischium, distal end, foot (= anteroposterior expansion): absent (0); present (1). (formerly 134)
93. Ischium, length relative to pubis length: subequal (0); at least 25% shorter (1). (Rowe, 1989) (Sereno, 1999; matrix 7, character 46)
94. Ischium, antitrochanter, nonarticular acetabular margin: concave (0); notch that undercuts antitrochanter (1). (Sereno, 1999; matrix 7, character 6)
95. Ischium, antitrochanter, anteroposterior length relative to adjacent length of the articular surface for the ilium: greater (0); less (1). (Sereno, 1999; matrix 7, character 7)
96. Puboischial symphysis (distal ends): absent (0); present (1). (formerly 38)
97. Puboischial contact below acetabulum (lateral view), depth relative to width of pubic peduncle of ischium: subequal (0); 25% or less (1). (formerly 39)
98. Pubis, pubic fenestra, partial or complete opening: absent (0); present (1). (Sereno, 1999; matrix 7, character 9)
99. Pubis, shaft axis (lateral view): straight (0); bowed anteriorly (1). (Rowe, 1989; (Sereno, 1999; matrix 7, character 50)
100. Pubis, prepubic process: absent (0); present (1). (formerly 41)
101. Pubis, obturator opening, form: foramen (0); notch (1). (formerly 40)
102. Pubis, shaft, orientation (lateral view): anteroventral (0); vertical (1); posteroventral (2). (formerly 35)
103. Pubis, shaft, shape: blade-shaped (0); rod-shaped (1). (formerly 36)
104. Pubis, symphysis, location: along entire pubic blade (0); at distal end only (1). (formerly 37)
105. Pubis, distal end of blade, transverse width relative to proximal blade: subequal (0); 65% or less (1). (formerly 95)
106. Pubis, distal end, foot (= distal anteroposterior expansion): absent (0); present (1). (loss of broad blade-shaped distal end) (formerly 101)
107. Pubis, foot, symphyseal area, location: none or limited to distal edge (0); broad median contact (1). (formerly 135)

Hind Limb

108. Femur, posterior aspect of head, ligament depression, shape: groove or shallow trough (0); broad fossa (1). (new character)
109. Femur, proximal shaft, anterolateral margin: rounded (0); crested (1). (formerly 104)
110. Femur, anterior trochanter, form: pyramidal prominence (0); fusiform (bullet-shaped) (1); flange-shaped (2). (formerly 43)
111. Femur, trochanteric shelf: absent (0); present (1). (Gauthier, 1986)
112. Femur, anterior trochanter, dimorphism: absent (0); present (1). (Sereno, 1999; matrix 7, character 10)
113. Femur, fourth trochanter, shape: crescentic, distal end variable corner (0); trapezoidal, proximal and distal corners (1); pendant distal margin (2). (formerly 44)
114. Femur, distal end, anterior attachment scar/fossa: absent (0); present (1). (formerly 102)
115. Tibia, proximal shaft, fibular crest: absent (0); present (1). (formerly 136)

116. Tibia-fibula, shafts, articular relation: separated (0); in articulation (1). (Gauthier 1986)
117. Tibia, distal end, posterolateral flange, lateral extension: does not reach fibula (0); extends posterior to medial margin of fibula (1); extends posterior to entire distal end of fibula and calcaneum (2). (formerly 45)
118. Tibia, distal end, lateral flange, shape (anterior view): subtriangular (0); tab-shaped with distinct proximolateral corner (1). (Sereno, 1999; matrix 7, character 42)
119. Fibula, minimum anteroposterior diameter at mid-shaft relative to maximum dimension of proximal end: 40% (0); 10-25% (1). (formerly 139)
120. Astragalus-calcaneum, suture and mutual processes: open, present (0); fused, absent (1). (Rowe, 1989; (Sereno, 1999; matrix 7, character 13)
121. Astragalus, fibular facet: present (0); absent (1). (formerly 46)
122. Astragalus, fibular facet, primary orientation: dorsolateral (0); lateral (1). (formerly 84)
123. Astragalus, (anterior) ascending process, fibular articulation, orientation: lateral (0); anterior (1). (new character)
124. Astragalus, (anterior) ascending process, shape: wedge-shaped (projecting into tibia) (0); plate-shaped (set in anteriorly facing tibial facet) (1). (formerly 71)
125. Astragalus, anteromedial corner, shape (dorsal view): subrectangular (0); anteriorly projecting at least 25% width of the medial side of the astragalus (1). (new character)
126. Astragalus, anterolateral process for calcaneum: present (0); absent (1). (formerly 15)
127. Astragalus, posteromedial crest (to posteromedial corner): absent (0); present (1). (formerly 141)
128. Calcaneum, medial process, size (correlated with width of distal articular surface): subtriangular flange (maximum width of distal articular surface greater than depth of lateral face) (0); rudimentary prominence (maximum width of distal articular surface subequal or less than depth of lateral face) (1). (formerly 16)
129. Calcaneum, posterior tuber: present (0); absent (1). (new character)
130. Calcaneum, fibular facet, form: flat or very gently concave (0); markedly concave (1). (new character)
131. Calcaneum, distal articular surface, form: flat (0); strongly dorsoventrally convex (1). (new character)
132. Distal tarsal 4, heel (projection posterior to ankle joints): present (0); absent (1). (formerly 49)
133. Metatarsal 1, length relative to metatarsal 2: more than 50% (0); less than 50% (1). (formerly 142)
134. Metatarsal 1, articular position on metatarsal 2: medial side, proximal half (0); posteromedial side, mid shaft (1). (formerly 143)
135. Metatarsals 2-4, basal articulation, dorsoventral overlap: minor (0); mt2 over mt3 over mt4 (1). (formerly 72)
136. Metatarsal 4, shaft axis, curvature (dorsal view): straight (0); sigmoid (curving away from mt3) (1). (formerly 118)
137. Metatarsal 4, distal end (and phalanx IV-1, base), proportions: broader than deep or subequal (0); deeper than broad (1). (formerly 144)
138. Metatarsal 5, length relative to metatarsal 3: 35-50% (0); less than 25% (1). (formerly 48)
139. Pedal digit V phalanges: absent (0); present (1). (formerly 47, reversed state assignments)

Matrix

MATRIX

DINOSAUROMORPH_ANC
00000000000000000000000000000X00000000000000000000000000?0000000000000000000000000000X000000000000000000X000000000X0000X00000000000000000

LAGERPETIDAE
??0????????????????????2000000000X00000XX00000000000X000(0 1)00000X0010X0X1X0X10001000000

Marasuchus
0??000000?????????????????????0?0???????????000??000000?000000?000?0?000?????????0000000000X00000000000000000X000100000000000X000000000000000

SILESAURIDAE 0000?0?000000000000???0????0?0???0000?00011(0 1)X10000000000000000000?000?????????00100000100000000000100000000X00210100000000000000000???00000

HETERODONTOSAURIDAE
00001010110001010001100011000000X11111011011101000000000001110001111112001100111101100011000000?00110011211X0X00200201020111X110??101110000010

Lesothosaurus
00001010000?0100000100000100000X11110021011101000000000001100001011?100000000011000000010100001100112 11X0X00200200020001X11010101110000010

GENASAURIA 00001010(0 1)00001010000000000100000X11111021011101000000000000110000111 1?10000000001101(0 1)000101?10000110011211X0X00200200020001X1101010111000(0 1)(0 1)10

Eoraptor 011000101000000000 1101?10000?0100000X10000(0 2)(0 1)10??000100100100 0?00000?2100010110201000001201010010000000000X000100000000001001?0?00000010000

Panphagia 01????????0??????????????????0X0000X1???0(0 2)(0 1)1???00010010???0?00??????????????20?0000012010100 10?000000000X0???0??000000001001?????????1????

Saturnalia
??????????????????????????????????0???????021????000100100010000?0?0?2???????????0?00000120101001000000000X0101010000000010010000000011100

SAUROPODIFORMES 011000010000000010110101(0 1)000000X0000X1000021110000(0 1)100100(0 1)(0 1)00000000?2100000110201010001001010000000000000X00100100000000100110100100010001

Herrerasaurus
00100?10000000000101010010000?110000X10000000110000100100100001 0?00112001110110000100000000000001001100101001000000000000000000000010001

Staurikosaurus
????????????????????????????????110000X????0000???000?00100??0001???01??????????00001010100000000?000?000110010 1?0100000?????????????????????

Eodromaeus
00?00?1000?0?00001?????0???0?1???000X?000000001010110010 0?000010?00112001110113000100012000100000010000011000010011000000000000000000000?00??

Tawa
0000010111?11010110001?010???0??0000X?0010000???101??01????0?01???01120111101 1?0?0100010???1?000001000001111001001000 0?0000001?11???00?0000

Coelophysis
10010?01111110101001011010 1??0100000X?00100001111021111111111110?00112111110113100111113000111100110000011110011011111110000011111101101100

Syntarsus_r.
10010?01111110101 0?10110101110100000X?00100001111?211111111111 10?00112111110113100111113000111100110000011110011011111110?0001?111101101100

'"Syntarsus" k.'
10010?01111110101101111?010????100000X?0010000???10?11????111?????011??????????31001
11113000??11??????????11100110111111110?0??X?1111?11?????
Dilophosaurus
?000010111111010110111001O?111100000X?0010000?111101101001l?10100001121111101131001
11013000101100000100O?11100110111101100010111111101111100
Ceratosaurus
?0100100001000001111110010111110000X1100000011111010010011?0100?0112111110?131001
00012000100000000100O?10002100111101100000X?1111???111??

6c. Comparative phylogenetic results

We focus our comparisons on the phylogenetic analyses of Sereno (1999) (*S24*) and the more recent analyses of Langer and Benton (2006) (*S25*), Nesbitt et al. (2009) (*S26*), and Ezcurra (2010) (*S13*) (Fig. S1). Several of these analyses incorporate terminal taxa far from the basal radiation of dinosaurs and thus also incorporate considerable character data irrelevant to basal relations. In order to facilitate comparison, we reduce the nondinosaurian outgroups and fragmentary or oversampled ingroup taxa to focus on the most relevant character evidence impacting relationships of the best known taxa at the base of Dinosauria (Table S5).

Sereno (1999) (*S24*)—This analysis used a composite dinosauromorph ancestor and *Marascuhus* as successive outgroups to 13 dinosaurian ingroups, 7 of which are suprageneric taxa. However, six characters in the original analysis are uninformative, (1, 2, 4, 5, 7, 9), and characters 59 and 83 are duplicates, reducing the total number of informative characters to 139. If we remove a pair of poorly known genera (*Pisanosaurus*, *Chindesaurus*) and two suprageneric taxa that sample more deeply than needed within Ornithischia (Ornithopoda, Marginocephalia), the number of informative characters drops to 128, which yield a single tree of 177 steps (CI = 0.84; RI = 0.86) (Fig. S1A). Importantly, two of the terminal taxa (Prosauropoda, Ceratosauria) are no longer widely regarded as monophyletic in their most inclusive interpretations. As a result, important character data that could have impacted basal relationships was located in separate analyses of these groups in this study. The new analysis incorporates this relevant character data.

Langer & Benton (2006) (*S25*)— This analysis used an allzero outgroup, ingroups composed of the dinosauriform *Silesaurus* and nine dinosaurian taxa, and 98 characters, of which 6 are ordered. Removing from the ingroups a pair of fragmentary genera (*Pisanosaurus*, *Guaibasaursus*), 96 of the original 98 informative characters remain informative (characters 18 and 19 now uniform), yielding a single tree of 179 steps (CI = 0.53; RI = 0.62) (Fig. S1B). Although *Eoraptor* and herrerasaurids are positioned at the base of Saurischia outside Theropoda and Sauropodomorpha, that relationship collapses with one additional step. Removing ordered character states collapses the relationship between *Silesaurus*, ornithischians and saurischians, but not the tenuous structure within Saurischia.

A gross comparison of character data after adjustments to maximize overlap shows highly significant differences between this analysis and the others considered (Table S6). Not only are there significantly fewer characters in the analysis pertaining to basal relationships, the percentage of cranial characters is half that in the analyses of Sereno (1999) and Nesbitt et al. (2009). Clearly character selection, some

acknowledged and much undocumented (*S29*), plays a major role in determining the phylogenetic results.

Nesbitt et al. (2009) (*S26*)—Using the basal archosauromorph *Erythrosuchus* as an outgroup, this analysis includes a very broad sampling of 40 ingroup species, only 23 of which are dinosaurs. They scored 315 characters, 14 of which are ordered. Several nondinosaurian ingroups have no effect on basal relationships within Dinosauria; others reside with substantial instability within Dinosauria as they are based known on very incomplete materials. As much as one-third of the character data are not relevant to relationships at the base of Dinosauria—the problem we aim to address in this paper. We therefore reduce the taxa and character data accordingly to limit the analysis to one that is more directly comparable to the one we perform in this paper.

Nesbitt et al. (2009) reported maximum parsimony analysis of 315 characters in 41 taxa, yielding three minimum-length trees of 872 steps, strict consensus of which shows a single polytomy among poorly known basal ornithischians (*S26*: Fig. S1). There are only 313 informative characters (characters 11 and 20 are uninformative). The same three trees are obtained with all characters unordered (now reduced to 869 steps); thus, ordering of the 14 characters, some of which mix absence with shape character states (*S27*), is not a factor in shaping the results.

There is great loss of resolution with increase in tree length. At one and two steps beyond minimum length, there are 44 and 340 trees, respectively. The position of *Eoraptor* an herrerasaurids, for example, loses resolution among saurischians with only one additional step. This loss of resolution is due in large measure to inclusion of very poorly known ingroup taxa, such as *Chindesaurus*. Deleting 11 taxa that lie outside Dinosauromorpha (2 pterosaurs 7 curotarsal archosaurs, 2 basal archosauromorphs) reduces the informative characters by one-third to 205, while yielding the same three minimum-length and strict consensus trees. We deleted seven additional ingroup taxa, four of which are very poorly known with better preserved kin among ingroups (*Eucoelophysis, Eocursor, Pisanosaurus, Chindesaurus)* and three of which are derived tetanuran theropods (*Piatnitzkyasaurus, Allosaurus, Velociraptor*). This reduces the informative characters and minimum tree length to 187 and 424, respectively, yielding three minimum-length trees with a polytomy among basal neotheropods.

Exploring the reduced tree shows that support for *Eoraptor* and *Herrerasaurus* as theropods is not particularly weak, as suggested by Nesbitt et al. (2009:1532). It takes six additional steps to break down Theropoda as a clade including *Hererrasaurus*, *Staurikosaurus* and *Eoraptor*—as many steps as was needed to link *Chindesaurus* with *Tawa*—a relationship they regarded as unlikely. The strength of the union between *Eoraptor*, herrerasaurids and neotheropods was masked more by unstable taxa than their conflictive character state scores.

Further reduction among nondinosaurian outgroups and the sampled diversity within Neotheropoda (by limiting dinosaurian outgroups to *Marasuchus* and by removing *Liliensternus, Cryolophosaurus, Zupaysaurus*) yields one shortest tree (341 steps) with 144 informative characters among basal dinosaurs. All nodes within this tree are stable with two additional steps; it takes five steps before *Eoraptor*, two herrerasaurids and other theropods collapse as a clade to include sauropodomorphs. These 144 characters comprise the majority of the informative character data in this analysis for the

early radiation of dinosaurs (Fig. S1C). The number and distribution of characters is grossly similar to the analysis of Sereno (1999) (Table S6).

Fig. S1. Cladograms showing relationships of principal taxa at the base of Dinosauria with reduction of dinosaurian outgroups, fragmentary taxa, and unnecessary neotheropod diversity. (**A**) Based on Sereno (1999). (**B**) Based on Langer and Benton (2006). (**C**) Based on Nesbitt et al. (2009). (**D**) Based on Ezcurra (2010).

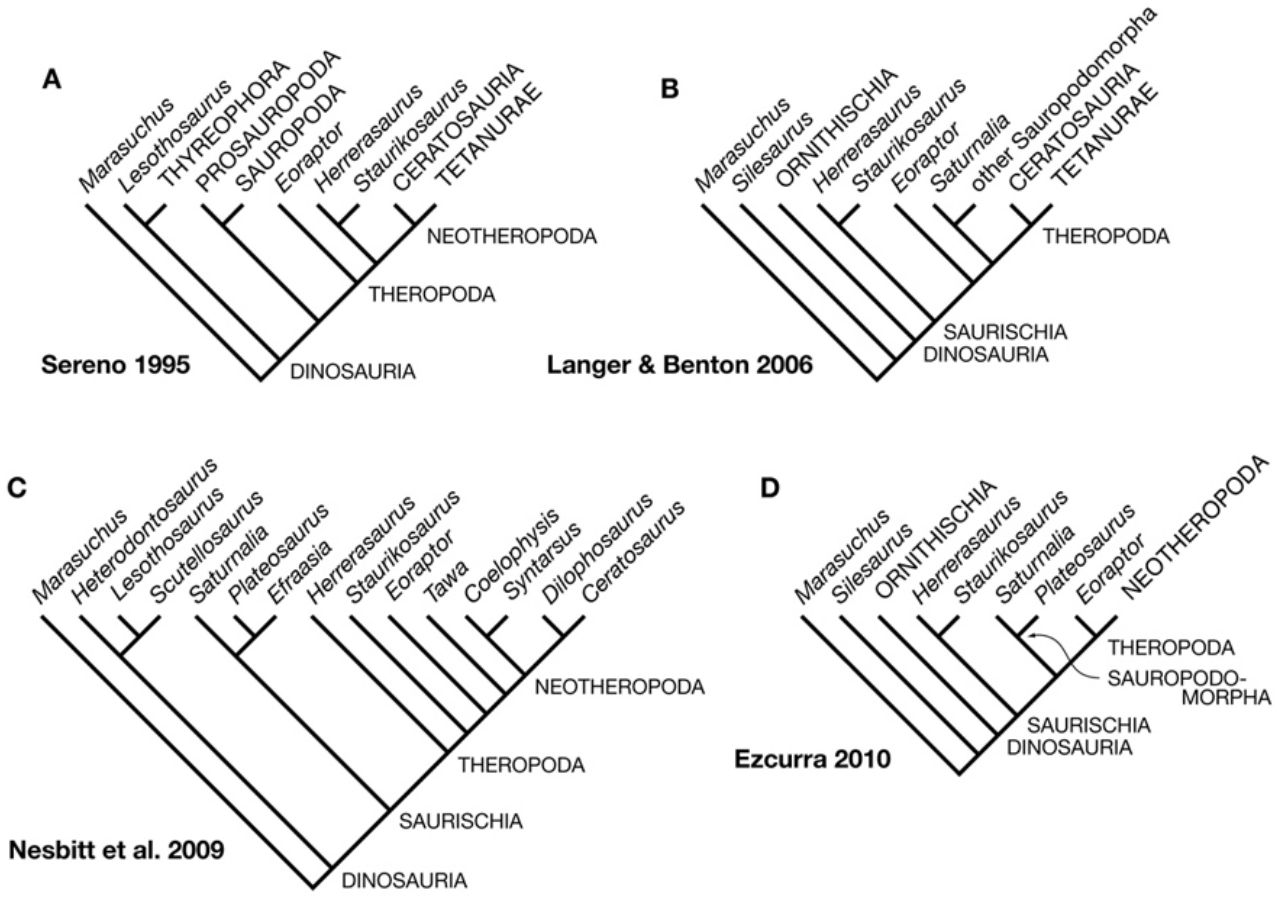

Table S6. Character counts after taxon reduction among three hypotheses for the basal radiation of Dinosauria.

Category	Sereno (1999)	Langer & Benton (2006)	Nesbitt et al. (2009)	Ezcurra (2010)
Total informative characters in published matrix	146	98	313	377
Informative characters after taxon reduction	128	96	144	139
Cranium	44 (35%)	20 (21%)	45 (31%)	30 (22%)
Dentition	7	6	6	7
Axial	20	19	22	28
Pectoral Girdle	1	—	2	3
Forelimb	14	20	17	14

Pelvic Girdle	25	14	21	27
Hind Limb	34	17	31	30

In the matrix of Nesbitt et al. (2009), several character states for *Eoraptor* and *Herrerasaurus* appear to be scored incorrectly. *Eoraptor* does not have a "subnarial gap" akin to that in coelophysoids (character 13). Just above the alveolar margin, *Eoraptor* has a subnarial foramen, the edges of which are slightly ajar on one side of the skull, as correctly diagrammed by Benton and Langer (*S25*). This is a foramen not an open gap between premaxilla and maxilla, as in *Dilophosaurus* and other coelophysoids. The ventral surface of the basisphenoid in *Eoraptor* is concave but is not deeply or distinctly recessed (character 69). This surface does not resemble the deep fissure that characterizes *Eodromaeus* and many theropods (Fig. 1C). Many of the crowns in *Eoraptor* show a distinct expansion above the root and a fairly sharp lateral crest on the crown (Fig. 1D), unlike *Eodromaeus* and most theropods that have flatter crowns that join their root without constriction (Fig. 1E) (character 111). The distal caudal vertebrae are preserved only to caudal 17 in the holotype of *Eoraptor*, which do not show any indication of elongate caudal prezygapophyses (character 149); *Panphagia* preserves more distal caudal vertebrae, which also do not have elongate prezygapophyses. We can score them as absent, as they are clearly present in *Eodromaeus* by caudal vertebrae 17. The pubic blade in *Eoraptor* forms a broad, plate-shaped apron without any development of a posteriorly directed foot, closely resembling the condition on basal sauropodomorphs; the distal breadth of the blade, however, was scored as unknown (character 208) and as having the form of a foot (character 207). *Herrerasaurus* has been shown recently to have a promaxillary fenestra (*S29*), which was scored as absent (character 27). The same is true for "*Syntarsus" kayentakatae* (*S30*), which unlike *Syntarsus rhodesiensis* also has a promaxillary fenestra.

These and other character state scores play an important role in the positioning *Eoraptor* within Theropoda closer to *Tawa* and neotheropods than herrerasaurids (*S25*). We argue that the theropod affinity of *Eoraptor* is illusory and is based primarily on misinterpretations and a suite of features in the manus (retractor pits on the heads of metacarpals 1-3, trenchant unguals) that now appear to be dinosaurian synapomorphies.

Ezcurra (2010) (*S13*)—Using *Euparkeria* as an outgroup, Ezcurra (2010) added 15 characters to data from previous analyses of sauropodomorph relationships (esp. *S32*) . In all 50 taxa were scored for 378 unordered characters, one of which (character 3) is parsimony uninformative (Table S6). Maximum parsimony analysis using PAUP yields a strict consensus of 100 minimum-length trees of 1186 steps as described (CI = 0.372; RI = 0.697). However, removal of *Euparkeria* and Crurotarsi among basal groups and scores of fragmentary or derived sauropodomorphs leaves relationships of remaining seven basal dinosaurs as in the consensus tree, while reducing the number of informative characters to 139 and the output of a single most parsimonious tree (393 steps; CI = 0.550; RI = 0.412). The information content regarding basal nodes within Dinosauria appears to be little altered. Two important nodes are shown with decay indices of 1 step; one additional step in the reduced analysis, however, does not break down the relations among retained taxa, probably the result of removal of several poorly known basal dinosaurs (*Chindesaurus*, *Guaibasaurus*). Two additional steps collapses

Ornithischia, Herrerasauridae, Sauropodomorpha, and Theropoda into an unresolved polytomy, with *Eoraptor* allied neotheropods.

As with the other analyses, there is very little decisive data at the base of Dinosauria and little way of knowing how that character data compares to that in other analyses, i.e., whether is has been incorporated and scored similarly. The promaxillary fenestra, for example, is not among the characters considered, although it has been described as a synapomorphy uniting in *Herrerasaurus* and many basal neotheropods (*S30*). The twist in the first phalanx of manus digit I (character 234), a feature associated with basal sauropodomorphs, was scored as unknown in *Eoraptor* (but see Fig. 1F).

Comparisons—The differences between the four hypotheses compared and the hypothesis in the present paper reside in the use of different characters (character selection) and in different character state scores for the same characters (character disparity, conflict and mismatch) (*S29*). A cursory examination of the character data as tabulated in Table S6 shows that character partitions differ significantly between the four hypotheses. Character selection, as a consequence, must pay a major role in generating different phylogenetic results. Sereno (1999) and Nesbitt et al. (2009) are the most comparable in terms of the total number of characters and the number of characters in different partitions. The other two hypotheses have 10% fewer cranial characters. A more detailed comparative analysis is underway (Sereno, in preparation) to quantify character selection and scoring between these hypotheses, which is beyond the scope of the present summary.

References

S1. J. P. Milana, O. Alcober, *Rev. Asoc. Geol. Argentina* **49**, 217 (1994).

S2. O. R. López-Gamundí, I. S. Espejo, P. J. Conaghan, C. M. A. Powell, J. J. Veevers, in *Permian-Triassic Pangean Basins and Fold Belts along the Panthalassan margin of western Gondwanaland,* J. J. Veevers, C. M. Powell, Eds. (Geological Society of America, Memoir, 1994), vol. 184, pp. 281-329.

S3. R. R. Rogers, C. C. S. III, P. C. Sereno, A. M. Monetta, R. N. Martinez, *Science* **260**, 794 (1993).

S4. N. J. Tabor *et al.*, in *Paleoenvironmental Record and Applications of Calcretes and Palustrine Carbonates,* A. A. Alonzo-Zarza, L. H. Tanner, Eds. (Geological Society of America, Special Papers, 2006), vol. 416, pp. 17-42.

S5. B. S. Currie, C. E. Colombi, N. J. Tabor, T. C. Shipman, I. P. Montanez, *J. So. Amer. Earth Sci.* **27**, 74 (2009)

S6. J. F. Bonaparte, *J. Vert. Paleo.* **2**, 362 (1982).

S7. R. M. Casamiquela, *Ameghiniana* **4**, 47 (1967).

S8. J. F. Bonaparte, *J. Paleontol.* **50**, 808 (1976).

S9. W. D. Sill, *Ameghiniana* **7**, 341 (1970).

S10. M. C. Langer, C. L. Schultz, **43**, 633 (2003).

S11. P. C. Sereno, C. A. Forster, R. R. Rogers, A. M. Monetta, *Nature* **361**, 64 (1993).

S12. R. N. Martinez, O. A. Alcober, *PLoS ONE* **4** (2009)

S13. M. Ezcurra, *J. Syst. Palaeontol.* **8**, 371 (2010).

S14. K. Min, R. Mundil, P. R. Renne, K. R. Ludwig, *Geochim Cosmochim Acta* **64**, 73 (2000).

S15. K. F. Kuiper *et al.*, *Science* **320**, 500 (2008).

S16. P. R. Renne, R. Mundil, G. Balco, K. Min, K. R. Ludwig, *Geochim Cosmochim Acta* **74**, 5349 (2010).

S17. P. R. Renne *et al.*, *Chem. Geol.* **145**, 117 (1998).

S18. P. R. Renne, W. S. Cassata, L. E. Morgan, *Quat. Geochron.* **4**, 288 (2009).

S19. P. R. Renne, K. B. Knight, S. Nomade, K. N. Leung, T. P. Lou, *Appl. Rad. Isotop.* **62**, 25 (2005).

S20. P. R. Renne, Z. D. Sharp, M. T. Heizler, *Chem. Geol.* **255**, 463 (2008).

S21. R. H. Steiger, E. Jäger, *Earth Planet. Sci. Lett.* **36**, 359 (1977).

S22. T. C. Shipman, Ph D Thesis, University of Arizona, Tuscon (2004).

S23. R. B. Irmis *et al.*, *Science* **317**, 358 (2007).

S24. P. C. Sereno, *Science* **284**, 2137 (1999).

S25. M. C. Langer, M. J. Benton, *J. Syst. Palaeontol.* **4**, 1 (2006).

S26. S. J. Nesbitt *et al.*, *Science* **326**, 1530 (2009).

S27. P. C. Sereno, *Cladistics* **23**, 565 (2007).

S28. P. C. Sereno, *Cladistics* (2009).

S29. P. C. Sereno, S. L. Brusatte, *J. Syst. Palaeontol.* **7**, 455 (2009).

S30. P. C. Sereno, *Hist. Biol.* **19**, 145 (2007).

S31. R. S. Tykoski, PhD thesis, University of Texas at Austin (2005).

S32. A. M. Yates, *Spec. Pap. Palaeontol.* **77**, 9 (2007).

S33. M. D. Ezcurra, F. E. Novas, *Hist. Biol.* **19**, 35 (2007).

S34. N. D. Smith, P. J. Makovicky, W. R. Hammer, P. J. Currie, *Zool. J. Linn. Soc.* **151**, 377 (2007).